ELSEVIER

# Vibrational spectra and theoretical calculations of *p*-chlorophenol in the electronically excited $S_1$ and ionic ground $D_0$ states

Jianhan Huang [a,c,*], Kelong Huang [a,*], Suqin Liu [a], Qiong Luo [a], Wenbih Tzeng [b]

[a] *College of Chemistry and Chemical Engineering, Central South University, Changsha 410083, China*
[b] *Institute of Atomic and Molecular Sciences, Academia Sinica, Taipei 10617, Taiwan*
[c] *The State Key Laboratory of Molecular Reaction Dynamics, Institute of Chemistry, Chinese Academy of Sciences, Beijing 100080, China*

## Abstract

With the good mass resolution ($m/\Delta m$) of about 650, the $^{35}Cl$ and $^{37}Cl$ isotopomers of *p*-chlorophenol have been separated successfully in our home made time of flight mass spectrometer (TOF-MS). One-color (1C), two-color (2C), resonant two-photon ionization (R2PI), and mass analyzed threshold ionization (MATI) spectra of the both isotopomers have been further recorded. Within the detection limit of our experiment, the band origins of the $S_1 \leftarrow S_0$ transition and the adiabatic ionization energies (IE) of $^{35}Cl$ and $^{37}Cl$ *p*-chlorophenol are measured to be the same. The band origins of the two isotopic species are determined to be $34813 \pm 2\,cm^{-1}$ by the 1C-R2PI experiment, and the adiabatic IE values are given to be $68094 \pm 15$ and $68104 \pm 5\,cm^{-1}$ by the 2C-R2PI and MATI methods for the two isotopomers of $^{35}Cl$ and $^{37}Cl$ *p*-chlorophenol. Analysis on the $S_1 \leftarrow S_0$ transition energy of *para* substituted phenols suggests that the band origins are all red shifted from phenol regardless of the nature of the substituent, while the inductive effect plays an important role for the $D_0 \leftarrow S_1$ transition process. The spectral properties of the two isotopomers in the electronically excited $S_1$ and ionic ground $D_0$ states are similar, whereas the vibrational frequencies of some modes are slightly different by a few wavenumbers, displaying the isotope effect.
© 2007 Elsevier B.V. All rights reserved.

*Keywords:* 1C-R2PI; 2C-R2PI; MATI; Band origin; IE; Isotope effect

## 1. Introduction

In recent years, phenol and substituted phenol have been the frequent subjects of experimental and theoretical work because of their significance in industry and environment. For example, chlorophenols (including *o*-, *m*-, and *p*-chlorophenol), as one of the most important organic intermediates, are widely used for the manufacture of pesticides, rubber, drugs, varnishes and dyestuffs. As they are high toxic and extremely difficult to degrade biologically, efficient removal of these organic compounds from wastewater has drawn significant concern [1]. First of all, investigations of their molecular structures and vibrational

spectra in the electronic ground $S_0$ state, electronically excited state, and ionic state are of great importance.

For *o*- and *m*-chlorophenol, laser induced fluorescence (LIF) and resonance enhanced multiphoton ionization (REMPI) spectroscopy have shown that there are two rotational conformers, *cis* and *trans* isomers, arising from the orientation of the hydroxyl group with respect to the chlorine atom at the *ortho* and *meta* position [2–5]. The band origins of *cis* and *trans* isomers of *o*-chlorophenol are determined to be $35889 \pm 5$ and $35706 \pm 5\,cm^{-1}$ [3], whereas the corresponding ones of *cis* and *trans m*-chlorophenol are measured to be $35776 \pm 1$ and $35894 \pm 1\,cm^{-1}$, respectively [2]. For *p*-chlorophenol, only one rotamer is detected, and its $S_1 \leftarrow S_0$ transition energy is given to be $34809.8\,cm^{-1}$ by the rotationally resolved LIF spectrum [6].

A lot of theoretical studies have been performed to elucidate the molecular structures and vibrational spectra of *p*-chlorophenol in the $S_0$ and electronically excited states [7–10],

---

Concerning the experimental studies, IR [11], dispersed and excitation LIF [6,12], one color $(1+1)$ resonant two-photon ionization (1C-R2PI) spectroscopy [13] have been conducted, and some vibrations of *p*-chlorophenol in the $S_0$ and $S_1$ states have been assigned successfully. To the best of our knowledge, the detailed spectroscopic features of this molecule in the ionic ground $D_0$ state are little concerned.

There are two substituted groups, hydroxyl and chlorine groups, on the benzene ring for chlorophenols, which can influence the electron density of the benzene ring through inductive and conjugated effects. Hence chlorophenols are also good models to expound substitution effects of the hydroxyl and chlorine groups for the benzene ring. The hydroxyl group donates electron to the benzene ring, whereas the chlorine atom withdraws electron from the ring through inductive effect. On the other hand, the oxygen atom of the hydroxyl group and the chlorine atom share their *p* electrons with the π electron of the benzene ring through conjugated effect. These interactions will bring on some changes on the geometric structures and vibrations in the specific electronic states. In addition, element of Cl has two isotopes, $^{35}Cl$ and $^{37}Cl$, correspondingly *p*-chlorophenol has two isotopomers, $^{35}Cl$ and $^{37}Cl$ *p*-chlorophenol, and their respective molecular weights are 128 and 130, respectively. If the mass resolution ($m/\Delta m$) of the time of flight mass spectrometer (TOF-MS) is good enough to separate these two isotopomers, their spectroscopic properties in the electronically excited $S_1$ and ionic ground $D_0$ states will be presented, and investigations of the isotope effect on the transition energies and vibrations are feasible. However, these important properties of *p*-chlorophenol in the $S_1$ and $D_0$ states are little touched on in the literature.

Generally, resonant two photon ionization (R2PI) is the typical scheme for REMPI spectroscopy [14–19], and it contains 1C-R2PI and two color $(1+1')$ resonant two photon ionization (2C-R2PI). The molecular structures and vibrational spectra of molecules in the $S_1$ state can be revealed by using the 1C-R2PI spectroscopic method. If the second laser is introduced, a photon of the first laser excites the molecule from the $S_0$ to the intermediate $S_1$ state, another photon of the second laser excites the molecule from the intermediate $S_1$ state to the ionization threshold. By scanning the laser wavelength of the second laser, the ionization energies (IE) of molecules will be obtained [20], and this scheme is defined as 2C-R2PI. Another kind of 2C-R2PI method includes a scan of the first laser while fixing the wavelength of the second laser [21], then the molecular structures and vibrational modes of molecules in the $S_1$ state will be characterized like 1C-R2PI spectrum. In particular, this 2C-R2PI method is more useful than 1C-R2PI scheme when the energy gap between the ionization threshold and the intermediate $S_1$ state is larger than that between the intermediate $S_1$ state and the ground $S_0$ state.

In the last two decades, zero kinetic energy (ZEKE) [22] spectroscopy has become an important spectroscopic technique to determine the ro-vibrationally resolved ionic spectra of molecules except for the precise adiabatic IE. This method involves excitation of the long-lived high *n* Rydberg neutrals and their subsequent ionization by a delayed pulsed electric field,

leading to a production of the ZEKE electrons in well-defined energy states. The latter developed mass analyzed threshold ionization (MATI) spectroscopy [23] detects the threshold ions rather than the ZEKE electrons, and is more applicable for clusters, van der Waals complex, and isotopes.

In this paper, we have predicted the optimized molecular geometries of the isotopomers of $^{35}Cl$ and $^{37}Cl$ *p*-chlorophenol in the $S_0$, $S_1$, and $D_0$ states by ab initio and density functional theory (DFT) calculations. With the good mass resolution of our TOF-MS, the 1C-R2PI, 2C-R2PI, and MATI spectra of $^{35}Cl$ and $^{37}Cl$ *p*-chlorophenol are further reported. The band origins of the $S_1 \leftarrow S_0$ excitation and the adiabatic IE are measured, and the assignments of vibrations in the $S_1$ and $D_0$ states are attempted. Comparing the band origins and IE of phenol with some other *para* substituted phenol, the substitution effect of the hydroxyl and chlorine groups are illustrated. According to the vibrations of phenol and *p*-chlorophenol, as well as the ones of $^{35}Cl$ and $^{37}Cl$ *p*-chlorophenol in the $S_1$ and $D_0$ states, the halogen effect and isotope effect are elucidated.

## 2. Experimental and computational methods

### 2.1. Experimental method

The experiments were performed with a TOF-MS described elsewhere [24]. The *p*-chlorophenol (Aldrich, 99% purity) sample was heated to about 90 °C to acquire sufficient vapor pressure and seeded into 2–3 bar of helium and expanded into the vacuum through a pulsed valve with a 0.5 mm diameter orifice. The pulsed valve was operated at 10 Hz with pulse duration of about 80 μs. The molecular beam was collimated by a skimmer located 15 mm downstream from the nozzle orifice.

The molecular excitation process was initiated by two independent tunable UV laser systems controlled by a delay/pulse generator (DG535). The first tunable dye laser (Lambda-Physik, Scanmate UV with BBO-I and BBO-III crystal; Fluorescence 548 and R590 dyes) was pumped by a pulsed frequency-doubled Nd:YAG laser (Quanta-Ray GCR-3). The dye laser output was frequency doubled and directed perpendicularly to the molecular beam. The second tunable UV laser (Lambda-Physik, Scanmate UV with BBO-III crystal; R590, R610 and R640 dyes) was pumped by another frequency-doubled Nd:YAG laser (Quanta-Ray LAB-150). A Fizeau-type wavemeter (New Focus 7711) was used to calibrate the wavelengths of both lasers.

The 2C-R2PI experiment was accomplished by fixing the excitation laser (the first laser) wavelength to a particular vibronic level in the $S_1$ state, while scanning the ionization laser (the second laser) from several hundred wavenumbers above to a few hundred wavenumbers below the ionization threshold of the molecule, and the total ion current is collected. In the MATI experiments, about 160 ns after the occurrence of the laser pulses, a pulsed electric field of −2.0 V/cm was switched on to reject the prompt ions. About 12.6 μs later, a second pulsed electric field of 130 V/cm was applied to field-ionize the Rydberg neutrals. The threshold ions were then accelerated and passed a field-free region before being detected by a dual-stacked microchannel plate detector.

## 2.2. Computational method

All ab initio and DFT calculations were performed by GAUSSIAN 03 program package [25]. The labeling of the carbon atoms is 1–6 around the ring and the substituents are numbered as $C_1$−OH and $C_4$−Cl, as shown in Fig. 1. The computational results can give information of the molecular geometries, total energies, and vibrational frequencies of $^{35}$Cl and $^{37}$Cl p-chlorophenol in the $S_0$, $S_1$, and $D_0$ states. The vibrational frequencies were scaled by 0.90 for the $S_1$ state (on the CIS/6-311++G** level) and 1.00 for the $D_0$ state (on the B3PW91/6-311++G** level) to correct the combined errors stemming from basis set incompleteness, the neglect of electron correlation, and the vibrational anharmoncity. The IE was obtained from the difference in the zero point energy level in the $D_0$ and $S_0$ states.

## 3. Results and discussion

### 3.1. Molecular geometries of p-chlorophenol in the $S_0$, $S_1$, and $D_0$ states: theoretical predictions

Changes of the bond lengths and bond angles of a molecule can be an obvious indicator to the changes of molecular structure. The experimental results of the structural parameters for p-chlorophenol in the $D_0$ state are unacquirable up to now. Accordingly we have performed theoretical calculations to predict the optimized molecular structure for p-chlorophenol. Table 1 lists the optimized bond lengths and bond angles of p-chlorophenol by the B3PW91/6-311++G**, CIS/6-311++G**, and B3PW91/6-311++G** methods in the $S_0$, $S_1$, and $D_0$ states, respectively. The results indicate that p-chlorophenol has a symmetry plane and belongs to the $C_s$ point group in the three states. As the hydroxyl and chlorine groups replace the hydrogen atoms on the ring, they will interact with the benzene ring through inductive and conjugated effects, leading to some changes of the surrounding electron density on the ring and hence the geometric structure of the molecule.
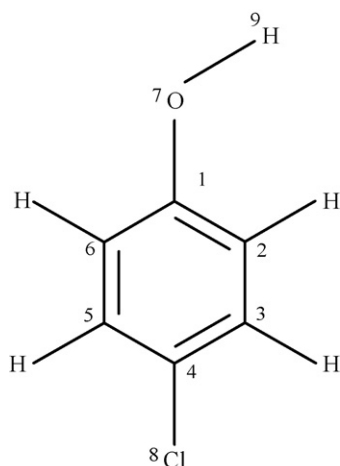


Fig. 1. The atom labeling of p-chlorophenol.

Table 1
The calculated structural parameters of p-chlorophenol in the $S_0$, $S_1$, and $D_0$ states by the B3PW91/6-311++G**, CIS/6-311++G**, and B3PW91/6-311++G** methods, respectively

| | $S_0$ | $S_1$ | $D_0$ |
|---|---|---|---|
| **Bond length (Å)** | | | |
| $C_1$−$C_2$ | 1.394 | 1.421 | 1.426 |
| $C_2$−$C_3$ | 1.388 | 1.403 | 1.364 |
| $C_3$−$C_4$ | 1.391 | 1.410 | 1.419 |
| $C_4$−$C_5$ | 1.388 | 1.408 | 1.422 |
| $C_5$−$C_6$ | 1.391 | 1.401 | 1.365 |
| $C_6$−$C_1$ | 1.394 | 1.413 | 1.424 |
| $C_1$−$O_7$ | 1.361 | 1.318 | 1.309 |
| $C_4$−$Cl_8$ | 1.747 | 1.720 | 1.686 |
| **Bond angle (°)** | | | |
| ∠$C_6C_1C_2$ | 119.8 | 122.3 | 121.0 |
| ∠$C_1C_2C_3$ | 120.1 | 118.8 | 119.5 |
| ∠$C_2C_3C_4$ | 119.8 | 118.1 | 119.4 |
| ∠$C_3C_4C_5$ | 120.6 | 123.0 | 121.3 |
| ∠$C_4C_5C_6$ | 119.6 | 118.9 | 119.5 |
| ∠$C_5C_6C_1$ | 120.2 | 118.4 | 119.4 |

The bond lengths of the ring CC bonds of p-chlorophenol are almost close to be 1.390 Å in the $S_0$ state, and the bond angles of the ring CCC are predicted to be about 120°. Upon the $S_1 \leftarrow S_0$ electronic excitation, the bond lengths of the ring CC are lengthened, while those of $C_1$−$O_7$ and $C_4$−$Cl_8$ bonds decrease from 1.361 and 1.747 Å in the $S_0$ state to 1.318 and 1.720 Å in the $S_1$ state, respectively. This indicates that the benzene ring is expanded on the $\pi^* \leftarrow \pi$ excitation of the benzene ring, whereas the interaction of the hydroxyl and chlorine groups with the ring is stronger in the $S_1$ state than that in the $S_0$ state. As for the bond angles, the angles of ∠$C_6C_1C_2$ and ∠$C_3C_4C_5$ are larger in the $S_1$ state than those in the $S_0$ state, whereas those of ∠$C_1C_2C_3$, ∠$C_2C_3C_4$, ∠$C_4C_5C_6$, and ∠$C_5C_6C_1$ are smaller in the $S_1$ state, which may be from the 1,4-substution of the hydroxyl and chlorine groups.

It has been noted that the transition from the neutral $S_1$ to $D_0$ state corresponds to the removal of the lone-paired electrons of the nitrogen atom for aniline and substituted aniline [26]. For phenol and substituted phenol, the $D_0 \leftarrow S_1$ electronic transition is similar to aniline and substituted aniline [27]. That is, the transition from the $S_1$ to $D_0$ state is subject to the removal of the lone-paired electrons of the oxygen atom of hydroxyl group. As a result, the remaining non-bounded electron on the oxygen atom will conjugate with the $\pi$ electron of the benzene ring, forming a partial C=O double bond. As can be seen in Table 1, the bond lengths of $C_1$−$O_7$ and $C_4$−$Cl_8$ bonds are further shortened on the $D_0 \leftarrow S_1$ transition, The bond length of $C_1$−$O_7$ bond is shorter than the C−O single bond length of 1.360 Å, and longer than the C=O double bond length of 1.230 Å. The shortened bond lengths of $C_1$−$O_7$ and $C_4$−$Cl_8$ bonds display a more rigid structure in the $D_0$ state with respect to that in $S_1$ state. As far as the ring CC bonds are concerned, the bond lengths of $C_2$−$C_3$ and $C_5$−$C_6$ bonds are shortened by 0.039 and 0.036 Å on the $D_0 \leftarrow S_1$ excitation, whereas the ones of $C_1$−$C_2$, $C_3$−$C_4$, $C_4$−$C_5$, and $C_6$−$C_1$ bonds are slightly lengthened. In this way, the benzene ring forms a configuration of two short bonds
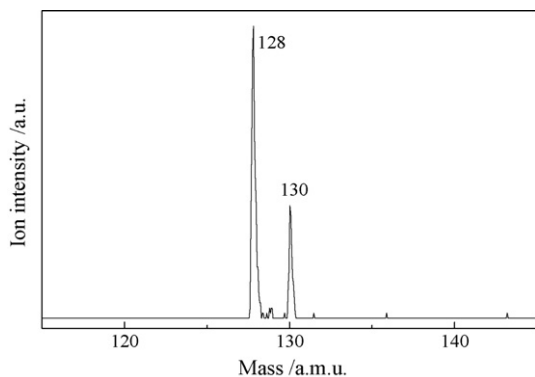
Fig. 2. TOF mass spectrum of *p*-chlorophenol recorded at the laser wavelength of 287.15 nm.

and four long bonds. The shortened bond lengths of $C_2-C_3$ and $C_5-C_6$ bonds show a more intense conjugation in the $D_0$ state corresponding to the presence of the partial C=O double bond illuminated above.

### 3.2. TOF mass spectrum of $^{35}Cl$ and $^{37}Cl$ isotopomers of p-chlorophenol

Element of Cl has two isotopes, $^{35}Cl$ and $^{37}Cl$. In our TOF spectrum of *p*-chlorophenol, there shows two peaks resulting from $^{35}Cl$ *p*-chlorophenol (*m/z*: 128) and $^{37}Cl$ *p*-chlorophenol (*m/z*: 130), as can be seen in Fig. 2. The peak at *m/z* 128 corresponds to a flight time of 26.32 μs with a full width at half maximum (FWHM) of 20 ns. This gives an estimated $t/\Delta t$ value of about 1300, corresponding to a mass resolution ($m/\Delta m$) of 650. This good mass resolvability warrants our success in recording the 1C-R2PI, 2C-R2PI, and MATI spectra of the selected isotopic species to be discussed below. In addition, the peak intensity ratio of $^{35}Cl$ and $^{37}Cl$ *p*-chlorophenol are close to be 3:1, corresponding to the natural abundance of $^{35}Cl$ and $^{37}Cl$.

### 3.3. 1C-R2PI spectra of $^{35}Cl$ and $^{37}Cl$ p-chlorophenol

*p*-Chlorophenol has 33 vibrations containing 30 benzene-like and 3OH group vibrational modes. Since the intensity of each vibronic band is related to the Franck-Condon overlaps, not all transitions are active. However, the well resolved vibronic features listed in the 1C-R2PI spectra might be referred to as the fingerprint states of the $^{35}Cl$ and $^{37}Cl$ isotopomers of *p*-chlorophenol. Fig. 3 shows the 1C-R2PI spectra of $^{35}Cl$ and $^{37}Cl$ *p*-chlorophenol in the energy range near the $S_1 \leftarrow S_0$ transition. The band origins of both isotopomers appear at 34813 cm$^{-1}$, with an inaccuracy of about ±2 cm$^{-1}$, in good agreement with that obtained from the LIF experiment [6,12]. The calculated total energies of $^{35}Cl$ and $^{37}Cl$ *p*-chlorophenol in the $S_0$ and $S_1$ states are listed in Table 2. The RHF/6-311++G** method is used for the calculation in the $S_0$ state, and the CIS/6-311++G** level is applied for the $S_1$ state. As shown in Table 2, the zero point energy level of $^{37}Cl$ *p*-chlorophenol is lower than that of $^{35}Cl$ *p*-chlorophenol by 7 cm$^{-1}$ for both of the $S_0$ and $S_1$ states, which predicts that the band origin of $^{37}Cl$ *p*-chlorophenol is the same as that of $^{35}Cl$ *p*-chlorophenol. Similar results
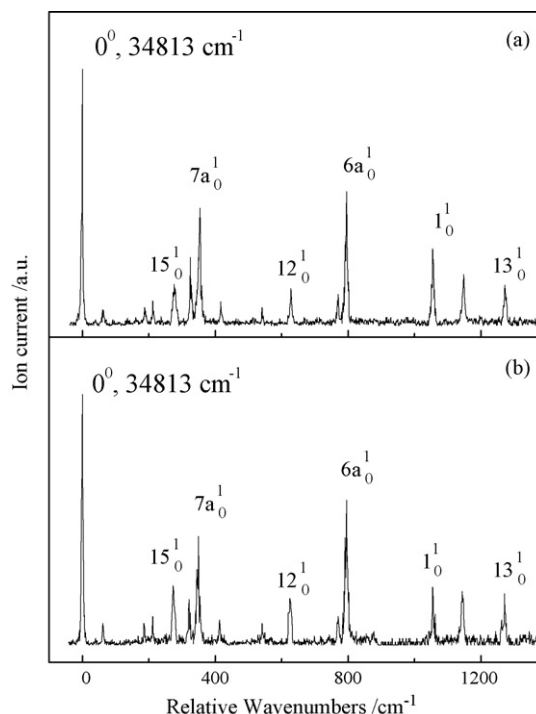


Fig. 3. 1C-R2PI spectra of $^{35}Cl$ and $^{37}Cl$ isotopomers of *p*-chlorophenol.

are reported for chlorobenzene [28] and *p*-chloroaniline [29]. CIS/6-311++G** calculation predicts the band origin of $^{35}Cl$ *p*-chlorophenol to be 42830 cm$^{-1}$, and that of the $^{37}Cl$ isotopomer also occurs at the same energy, supporting our experimental results.

According to Varsanyi [30], *p*-chlorophenol is classified as the 1-light-4-heavy di-substituted benzene. The numbering system of the benzene-like vibrations for *p*-chlorophenol is different from that for *p*-fluorophenol, which is classified as the 1,4-dilight di-substituted benzene. We assign the vibrational bands in the

Table 2
The calculated energies of $^{35}Cl$ and $^{37}Cl$ *p*-chlorophenol in the $S_0$, $S_1$, and $D_0$ states on the RHF/6-311++G**, CIS/6-311++G**, and UHF/6-311++G** levels, respectively

|  | $^{35}Cl$ *p*-chlorophenol | $^{37}Cl$ *p*-chlorophenol |
|---|---|---|
| **In the $S_0$ state** | | |
| $E_{RHF}$ | −764.562893 | −764.562893 |
| Zero point   correction | 0.101307 | 0.101275 |
| $E''$ | −764.461587 | −764.461618 |
| $\Delta E''$ (cm$^{-1}$) | 7 | |
| **In the $S_1$ state** | | |
| $E_{CIS}$ | −764.550395 | −764.550395 |
| Zero point correction | 0.096696 | 0.096665 |
| $E'$ | −764.258553 | −764.258583 |
| $\Delta E'$ (cm$^{-1}$) | 7 | |
| **In the $D_0$ state** | | |
| $E_{UHF}$ | −764.296732 | −764.296732 |
| Zero point correction | 0.100524 | 0.100492 |
| $E^+$ | −764.196208 | −764.196240 |
| $\Delta E^+$ (cm$^{-1}$) | 7 | |

$E''$, $E'$, and $E^+$ are the energies of the $S_0$, $S_1$, and $D_0$ states at the zero point energy level. 1 Hartree = 27.2116 eV = 219474.6 cm$^{-1}$.

Table 3
The observed vibrational bands (in cm$^{-1}$) of $^{35}$Cl and $^{37}$Cl isotopomers of *p*-chlorophenol in the 1C-R2PI spectra and possible assignments[a]

| Ref [12] | | This work | | | | |
|---|---|---|---|---|---|---|
| | | $^{35}$Cl *p*-chlorophenol | | $^{37}$Cl *p*-chlorophenol | | |
| Exp. | Assignments | Exp. | Cal. | Exp. | Cal. | Possible assignments and descriptions [b] |
| | | 63 | 81 | 62 | 80 | $11^1_0$, $\gamma$ (CC) |
| 191 | $11^2_0$ | 188 | | 186 | | $11^2_0$ |
| 265 | $\beta$ (C–Cl) | 277 | 265 | 273 | 263 | $15^1_0$, $\beta$ (C–Cl) |
| 317 (315) | $16a^2_0$ | 325 | | 322 | | $16a^2_0$ |
| 355 (351) | $6a^1_0$ | 354 | 342 | 349 | 342 | $7a^1_0$, $\nu$ (C–OH)/(C–Cl) |
| | | 417 | 397 | 413 | 397 | $9b^1_0$, $\beta$ (C–OH) |
| | | 628 | 604 | 625 | 602 | $12^1_0$, $\beta$ (CCC) |
| | | 770 | 764 | 770 | 764 | $10a^1_0$, $\gamma$ (CC) |
| 799 | $1^1_0$ | 796 | 792 | 796 | 792 | $6a^1_0$, $\beta$ (CCC) |
| 1069 | $\nu$ (C–Cl) | 1055 | 1039 | 1055 | 1038 | $1^1_0$, breathing |
| | | 1148 | 1121 | 1144 | 1121 | $9a^1_0$, $\beta$ (CH) |
| 1269 | $\nu$ (C–OH) | 1272 | 1282 | 1271 | 1282 | $13^1_0$, $\nu$ (C–OH) |

[a] The experimental values are shifted from 34813 cm$^{-1}$, whereas the calculated ones are obtained from the CIS/6-311++G** calculations, scaled by 0.90.

[b] $\nu$, $\beta$, and $\gamma$ represent stretching, in-plane bending and out-of-plane bending vibrations, respectively.

$S_1$ state by means of comparing these vibrational frequencies with those of this molecule in the $S_0$ state [11], and those of Ref. [12] in the $S_1$ state, as well as the calculated values from the CIS/6-311++G** calculation. When scaled by 0.90, the predicted frequencies in our calculation become very close to the measured ones. The GAUSSIAN VIEW program, which is a complementary program of GAUSSIAN 03 package, can view the normal vibrations of the calculated results [25]. We use it to check our assignment. All of the observed 1C-R2PI bands and their possible assignments of $^{35}$Cl and $^{37}$Cl isotopomers of *p*-chlorophenol are summarized in Table 3, the observed vibrational bands in Ref. [12] are also included.

The intense bands at 796 and 1055 cm$^{-1}$ for both $^{35}$Cl and $^{37}$Cl isotopomers in Fig. 3 are assigned to transitions $6a^1_0$ and $1^1_0$, which involve the in-plane ring deformations, and $1^1_0$ is usually referred to as the breathing motion, as seen in Fig. 4. The vibrational frequencies of these two modes in the $S_0$ state are reported to be 836 and 1094 cm$^{-1}$ [11]. The red shifts of these two modes in the $S_1$ state with respect to those in the $S_0$ state imply the expansion of benzene ring is taken place upon the $S_1 \leftarrow S_0$ excitation, consistent with the analysis of the optimized molecular geometries stated above. Mode 7a represents a coupled motion of the ring-substituent stretching C–OH/C–Cl and the ring deformation, which occurs at 354 and 349 cm$^{-1}$ for $^{35}$Cl and $^{37}$Cl *p*-chlorophenol, respectively.

The moderate bands at 277, 417, 628, 1148, and 1272 cm$^{-1}$ for $^{35}$Cl *p*-chlorophenol, and 273, 413, 625, 1144, and 1271 cm$^{-1}$ for $^{37}$Cl *p*-chlorophenol, are assigned to $15^1_0$, $9b^1_0$, $12^1_0$, $9a^1_0$, and $13^1_0$ transitions, respectively. These modes are related to the substituent sensitive in-plane C–Cl bending, in-plane C–OH bending, the ring deformation, the ring CH in-plane bending, and C–OH stretching, respectively. The weak bands at 63 and 770 cm$^{-1}$ (for $^{35}$Cl *p*-chlorophenol), 62 and 770 cm$^{-1}$ (for $^{37}$Cl *p*-chlorophenol), result from the out of plane bending motions of $11^1_0$ and $10a^1_0$.

### 3.4. 2C-R2PI and MATI spectra $^{35}$Cl and $^{37}$Cl *p*-chlorophenol

We have applied both 2C-R2PI and MATI techniques to locate the ionization limit of $^{35}$Cl and $^{37}$Cl *p*-chlorophenol. Fig. 5 shows the photoionization efficiency curves of $^{35}$Cl and $^{37}$Cl *p*-chlorophenol obtained via the $S_1 0^0$ state. Analysis on the rising step of the 2C-R2PI spectra gives the IE to be 68094 ± 15 cm$^{-1}$, and the IE for both isotopomers are the same. MATI method has



7a, $\nu$(C-Cl)/(C-OH)
$S_1$, 354 (350) cm$^{-1}$
$D_0$, 374 (369) cm$^{-1}$

12, $\beta$(CCC)
$S_1$, 628 (625) cm$^{-1}$
$D_0$, 655 (655) cm$^{-1}$

6a, $\beta$(CCC)
$S_1$, 796 (796) cm$^{-1}$
$D_0$, 819 (817) cm$^{-1}$

1, breathing
$S_1$, 1055 (1055) cm$^{-1}$
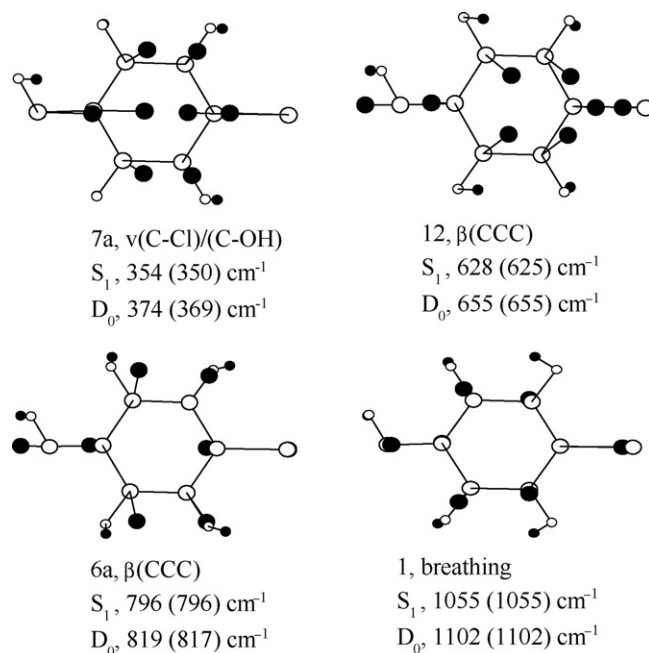$D_0$, 1102 (1102) cm$^{-1}$

Fig. 4. Some normal vibrations of *p*-chlorophenol. The open circles designate the original locations of the atoms, whereas the solid dots mark the displacements. The measured frequencies of $^{35}$Cl *p*-chlorophenol and $^{37}$Cl *p*-chlorophenol (in the parentheses) are included for each mode.
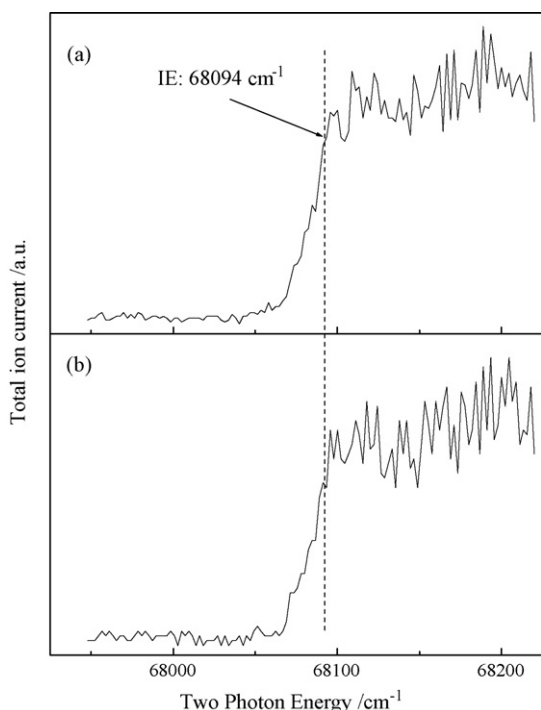
Fig. 5. 2C-R2PI spectra of $^{35}$Cl and $^{37}$Cl *p*-chlorophenol by ionizing via the $S_1 0^0$ state.
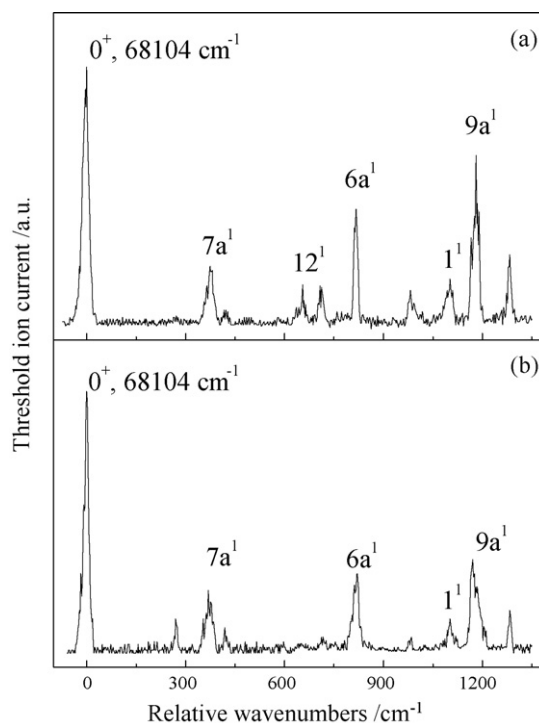


Fig. 6. MATI spectra of $^{35}$Cl and $^{37}$Cl isotopomers of *p*-chlorophenol recorded via the $S_1 0^0$ state.

also been used to determine the ionization threshold recorded by ionizing via the $S_1 0^0$, $S_1 7a^1$, and $S_1 6a^1$ states, and the IE values are shown in Table 4. Since MATI spectroscopy involves ionization of molecules in high *n* Rydberg states by a delayed pulsed electric field, the observed ionization threshold is slightly lower than that of the true one due to the Stark effect. The field-corrected adiabatic IE of the selected $^{35}$Cl and $^{37}$Cl *p*-chlorophenol by the three intermediate states are the same, with a value of $68104 \pm 5\,cm^{-1}$, in agreement with the value from the 2C-R2PI experiment. Table 4 also displays the calculated IE by the HF, B3LYP, and B3PW91 methods with the 6-311++G* and 6-311G++G** basis set. It can be seen that the B3PW91/6-311++G** method gives a better prediction for the IE with a smaller deviation of −2.2%.

The calculated energies of $^{35}$Cl and $^{37}$Cl *p*-chlorophenol in the $S_0$ and $D_0$ states are shown in Table 2. The RHF/6-311++G** method is used for the $S_0$ state, whereas the UHF/6-311++G**

level is applied for the $D_0$ state. As seen in Table 2, the zero point energy level of the $^{37}$Cl isotopomer is lower than that of the $^{35}$Cl isotopomer by about $7\,cm^{-1}$ for the $S_0$ and $D_0$ state, which implies the IE of the $^{37}$Cl isopotomer is the same as that of the $^{35}$Cl isopotomer. The transition from the neutral to the $D_0$ state corresponds to the removal of the lone-paired electrons of the oxygen atom of the OH group for phenols, but no changes occur on the "nucleus" of the molecule, and hence the same IE for the two isotopomers.

Fig. 6 displays the MATI spectra of $^{35}$Cl and $^{37}$Cl *p*-chlorophenol via the $S_1 0^0$ state. All of the observed vibrational bands in Fig. 6 and their possible assignments are listed in Table 5, along with the calculated frequencies by the B3PW91/6-311++G** method (with no scaling factor). The bands related to the benzene like vibrations are labeled according to Varsanyi's notations [30]. From the assignments of the vibrational bands in Fig. 6, it is known that most of the active vibrations of $^{35}$Cl and $^{37}$Cl *p*-chlorophenol in the $D_0$ state are related to the in-plane ring and substituent-sensitive modes. The bands resulted from the in-plane ring deformation vibrations 12, 6a, and 1 appear at 655, 819 (817), and $1102\,cm^{-1}$ for $^{35}$Cl and $^{37}$Cl *p*-chlorophenol species, respectively. As stated previously, vibrations 12, 6a, and 1 of $^{35}$Cl *p*-chlorophenol in the $S_1$ state appear at 628 (625), 796, and $1055\,cm^{-1}$, respectively. The blue shifts of these three modes suggest the more rigid configuration in the $D_0$ state. Vibration 7a occurs at 374 and $369\,cm^{-1}$ for $^{35}$Cl and $^{37}$Cl *p*-chlorophenol, respectively. The bands with frequencies at 422, 978, 1181, and $1283\,cm^{-1}$ for $^{35}$Cl *p*-chlorophenol, and 419, 978, 1171, and $1283\,cm^{-1}$ for $^{35}$Cl *p*-chlorophenol, concern the vibrations $9b^1$, $18a^1$, $9a^1$, and $14^1$, respectively.

Table 4
The experimental and calculated IE (in $cm^{-1}$) of $^{35}$Cl and $^{37}$Cl *p*-chlorophenol

| Methods | $^{35}$Cl *p*-chlorophenol | $^{37}$Cl *p*-chlorophenol | Dev (%) |
|---|---|---|---|
| 2C-R2PI (via $S_1\ 0^0$) | 68094 | 68094 | |
| MATI (via $S_1\ 0^0$) | 68104 | 68104 | 0 |
| MATI (via $S_1\ 7a^1$) | 68104 | 68104 | 0 |
| MATI (via $S_1\ 6a^1$) | 68104 | 68104 | 0 |
| HF/6-311++G* | 58156 | 58156 | −14.6 |
| HF/6-311++G** | 58244 | 58244 | −14.5 |
| B3LYP/6-311++G* | 66420 | 66420 | −2.5 |
| B3LYP/6-311++G** | 66534 | 66533 | −2.3 |
| B3PW91/6-311++G* | 66477 | 66476 | −2.5 |
| B3PW91/6-311++G** | 66593 | 66592 | −2.2 |

Table 5
Observed vibrational bands of $^{35}$Cl and $^{37}$Cl p-chlorophenol in MATI spectra and assignments[a]

| $^{35}$Cl p-chlorophenol | | | $^{37}$Cl p-chlorophenol | | | Assignments and approximate descriptions[b] |
|---|---|---|---|---|---|---|
| Exp. | Intensity | Cal. | Exp. | Intensity | Cal. | |
| 0 | 100 | | 0 | 100 | | $0^+$ |
| | | 276 | 270 | 13 | 276 | $15^1$, β (C—Cl) |
| 374 | 23 | 387 | 369 | 24 | 382 | $7a^1$, ν (C—OH)/(C—Cl) |
| 422 | 6 | 428 | 419 | 10 | 425 | $9b^1$, β (C—OH) |
| 655 | 16 | 672 | 655 | 4 | 669 | $12^1$, β (CCC) |
| 712 | 15 | | | | | $15^1 9b^1$ |
| 819 | 45 | 836 | 817 | 30 | 835 | $6a^1$, β (CCC) |
| 978 | 14 | 992 | 978 | 5 | 992 | $18a^1$, β (CH) |
| 1102 | 18 | 1129 | 1102 | 13 | 1129 | $1^1$, breathing |
| 1181 | 66 | 1207 | 1171 | 36 | 1207 | $9a^1$, β (CH) |
| 1283 | 27 | 1303 | 1283 | 12 | 1303 | $14^1$, ν (CC) |

[a] The experimental values are shifted from 68104 cm$^{-1}$, whereas the calculated ones are obtained from B3PW91/6-311++G** calculations with no scaling.

[b] ν, stretching; β, in-plane bending; γ, out-of-plane bending.

## 3.5. Substitution effect of para substituted phenol derivatives on the transition energy

Table 6 summarizes the band origins of the $S_1 \leftarrow S_0$ excitation and the adiabatic IE of phenol and its para substituted derivatives from R2PI, ZEKE, and MATI experiments [27,31–37]. The band origins of para substituted phenols are all red shifted from phenol regardless of the nature of the substituent, which suggests that the interaction of the substituents with the ring is stronger in the $S_1$ state than that in the $S_0$ state [38,39]. For p-chlorophenol, the red shift of the transition energy in the $S_1 \leftarrow S_0$ excitation implies the interaction of the hydroxyl and chlorine groups with the ring is stronger, in agreement with

the analysis from the optimized geometric structure. In addition, the OH, OCH$_3$, and NH$_2$ groups not only donate electrons to the ring through σ bond, but interact with the ring through π orbital, leading to a greater energy red shift.

As shown in Table 6, the transition energy of the $D_0 \leftarrow S_1$ process of p-fluorophenol, p-chlorophenol, and p-cyanophenol are blue shifted from phenol, while the other para substituted phenols are red shifted. The electron-withdrawing F, Cl, and CN substituents reduce the electron density around the ring and hence the oxygen atom. As a result, the $D_0 \leftarrow S_1$ transition energies of p-fluorophenol, p-chlorophenol, and p-cyanophenol are higher than that of phenol, In contrast, the other electron-donating substituents such as CH$_3$, OH, OCH$_3$, and NH$_2$ groups

Table 6
Measured transition energies of phenol and its para substituted derivatives[a]

| Molecule | $S_1 \leftarrow S_0$ | $\Delta E_1$ | $D_0 \leftarrow S_1$ | $\Delta E_2$ | IE | $\Delta$IE |
|---|---|---|---|---|---|---|
| Phenol[b] | 36349 | 0 | 32276 | 0 | 68625 | 0 |
| p-Methylphenol[c] | 35331 | −1018 | 30587 | −1689 | 65918 | −2707 |
| p-Ethylphenol[c] | 35504 | −845 | 30124 | −2152 | 65628 | −2997 |
| trans-p-n-Propylphenol[d] | 35501 | −848 | 29782 | −2494 | 65283 | −3342 |
| gauche-A p-n-Propylphenol[d] | 35453 | −896 | 29932 | −2344 | 65385 | −3240 |
| gauche-B p-n-Propylphenol[d] | 35441 | −908 | 29928 | −2348 | 65369 | −3256 |
| trans-Hydroquinone[e] | 33500 | −2849 | 30498 | −1778 | 63998 | −4627 |
| cis-Hydroquinone[e] | 33535 | −2814 | 30516 | −1760 | 64051 | −4575 |
| trans-p-Methoxyphenol [f] | 33572 | −2777 | 28638 | −3638 | 62210 | −6415 |
| cis-p-Methoxyphenol [f] | 33667 | −2682 | 28646 | −3630 | 62313 | −6312 |
| p-Aminophenol [g] | 31393 | −4956 | 27429 | −4847 | 58822 | −9803 |
| p-Fluorophenol [h] | 35117 | −1232 | 33460 | 1184 | 68577 | −48 |
| $^{35}$Cl p-chlorophenol[i] | 34813 | −1536 | 33292 | 1016 | 68104 | −521 |
| $^{37}$Cl p-chlorophenol[i] | 34813 | −1536 | 33292 | 1016 | 68104 | −521 |
| p-Cyanophenol[j] | 35548 | −801 | 37152 | 4876 | 72700 | 4075 |

[a] $\Delta E_1$, $\Delta E_2$ and $\Delta$IE are shifted of $S_1 \leftarrow S_0$, $D_0 \leftarrow S_1$ and IE with respect to those of phenol.

[b] Ref [31].

[c] Ref [27].

[d] Ref [32].

[e] Ref [33].

[f] Ref [34].

[g] Ref [35].

[h] Ref [36].

[i] This work.

[j] Ref [37].

increase the electron density in the neighborhood of the ring and the oxygen, leading to the lower $D_0 \leftarrow S_1$ transition energies. As regards *p*-chlorophenol, the red shifted magnitude of the band origin is a little greater than that of the blue shift in the $D_0 \leftarrow S_1$ transition energies. Therefore, the IE of *p*-chlorophenol is lower than that of phenol by $521 \, cm^{-1}$. Analysis on the energy shifts suggests that the inductive effect plays an important role for the $D_0 \leftarrow S_1$ transition process for these *para* substituted phenols.

## 3.6. Halogen effect and isotope effect on the vibrations

In the $S_0$ state, vibrations 6a and 1 were measured to be 526 and $810 \, cm^{-1}$ for phenol [40], and 836 and $1094 \, cm^{-1}$ for *p*-chlorophenol [11]. In the $S_1$ state, the corresponding ones are found to be 475 and $935 \, cm^{-1}$ for phenol [31], and 796 and $1055 \, cm^{-1}$ for *p*-chlorophenol. In the $D_0$ state, the vibrational frequencies of these two modes appear at 521 and $973 \, cm^{-1}$ for phenol [31], and 819 (817) and $1102 \, cm^{-1}$ for *p*-chlorophenol. These data indicate that *p*-chloro substitution on phenol causes an increase in the vibrational frequency for these in-plane ring deformation modes. Because the chlorine atom is defined as the heavy atom, and it takes part in these two in-plane ring vibrations. The extent of the frequency increasing may be considered as the degree of the chlorine atom participates in the overall vibration. In addition, comparing the vibrational frequencies of vibrations 6a and 1 of in the $S_0$, $S_1$, and $D_0$ states, we can conclude that the vibrational frequencies in the $S_1$ state are less than those in the $S_0$ and $D_0$ state. Since the vibrational frequency is proportional to the square root of force constant, the greater vibrational frequency is, the stiffer chemical bond for a diatomic molecule is. In the case of a polyatomic molecule, a greater vibrational frequency implies a more rigid structure. The present experimental findings suggest that *p*-chlorophenol is more rigid in the $D_0$ state than in the $S_1$ state.

There is no difference for the band origins and IE for the both isotopomers of $^{35}Cl$ and $^{37}Cl$ *p*-chlorophenol. However, it is expected that the isotope effect will be seen in some vibrations when the chlorine atom takes part in the motion of the vibrations. For mode 1, the frequencies for the two isotopomers is the same in the $S_1$ state and $D_0$ state. For some other vibrations, such as vibrations 7a, 9b, 12, and 9a, the frequency difference between the $^{35}Cl$ and $^{37}Cl$ isotopomers of *p*-chlorophenol is about $1–4 \, cm^{-1}$ in the $S_1$ state and $3–10 \, cm^{-1}$ in the $D_0$ state, displaying the isotope effect.

## 4. Conclusion

With the good mass resolution of the TOF-MS, the 1C-R2PI, 2C-R2PI, and MATI spectroscopy of $^{35}Cl$ and $^{37}Cl$ *p*-chlorophenol in the $S_1$ and $D_0$ states have been recorded. The band origins and IE of the both isotopic species are found to be the same, with the values of 34,813 and $68,104 \, cm^{-1}$. Comparing the band origins and IE of phenol with those of *para* substituted phenol leads the following results. The band origins of *para* substituted phenols are all red shifted with respect to that of phenol. The transition energy of the $D_0 \leftarrow S_1$ process of the *p*-fluorophenol, *p*-chlorophenol, and *p*-cyanophenol are

blue shifted with respect to that of phenol, whereas the other *para* substituted phenols are red shifted. The inductive effect plays an important role in the $D_0 \leftarrow S_1$ transition.

The general properties in the vibronic and ionic spectra of both isotopomers are similar. Comparison of the vibrational frequencies of phenol and *p*-chlorophenol indicates *p*-chloro substitution causes an increase in the vibrational frequency for the in-plane ring deformation modes. Analysis on the vibrations shows that frequencies of some vibrational modes of $^{35}Cl$ and $^{37}Cl$ *p*-chlorophenol are slightly different by $1–4 \, cm^{-1}$ in the $S_1$ state and $3–10 \, cm^{-1}$ in the $D_0$ state, exhibiting the isotope effect.

## References

[1] U. Stafford, K.A. Gray, P.V. Kamat, A. Varma, Chem. Phys. Lett. 205 (1993) 55.
[2] S. Nakagawa, Y. Matsushita, T. Suzuki, T. Ichimura, J. Mol. Struct. 779 (2005) 68.
[3] S. Yamamoto, T. Ebata, M. Ito, J. Phys. Chem. 93 (1989) 6340.
[4] A. Oikawa, H. Abe, N. Mikami, M. Ito, J. Phys. Chem. 88 (1984) 5180.
[5] M.C.R. Cockett, M. Takahashi, K. Okuyama, K. Kimura, Chem. Phys. Lett. 187 (1991) 250.
[6] M. Böhm, C. Ratzer, M. Schmitt, J. Mol. Struct. 800 (2006) 55.
[7] W. Zierkiewicz, D. Michalska, Z.H. Theïre'se, J. Phys. Chem. A 104 (2000) 11685.
[8] D.S. Ahn, S.W. Park, S.Y. Lee, B.S. Kim, J. Phys. Chem. A 107 (2003) 131.
[9] J. Han, R.L. Deming, F.M. Tao, J. Phys. Chem. A 108 (2004) 7736.
[10] P. Imhof, D.K. Gler, R. Brause, K. Kleinermanns, J. Chem. Phys. 121 (2004) 2598.
[11] C. Garrigou-Lagrange, J.M. Lebas, M.L. Josien, Spectrochim. Acta. A 12 (1958) 305.
[12] P. Imhof, K. Kleinermanns, Phys. Chem. Chem. Phys. 4 (2002) 264.
[13] J. Huang, J.L. Lin, W.B. Tzeng, Chem. Phys. Lett. 422 (2006) 271.
[14] J.G. Philis, Spectrochim. Acta A 61 (2005) 1239.
[15] Y. Huang, M. Sulkes, Chem. Phys. Lett. 254 (1996) 242.
[16] A. Hirano, H. Tsumanuma, K. Kishi, T. Egawa, J. Mol. Struct. 701 (2004) 9.
[17] J.G. Philis, J. Mol. Spectrosc. 232 (2005) 26.
[18] T. Egawa, T. Yamada, S. Konaka, Chem. Phys. Lett. 324 (2000) 260.
[19] J.G. Philis, E. Drougas, A.M. Kosmas, Chem. Phys. 306 (2004) 253.
[20] D. Bellert, W.H. Breckenridge, Chem. Phys. Lett. 337 (2001) 103.
[21] C. Wu, Y. He, W. Kong, Chem. Phys. Lett. 398 (2004) 351.
[22] K. Müller-Dethlefs, M. Sander, E.W. Schlag, Chem. Phys. Lett. 112 (1984) 291.
[23] L. Zhu, P.M. Johnson, J. Chem. Phys. 94 (1991) 5769.
[24] W.B. Tzeng, J.L. Lin, J. Phys. Chem. A 103 (1999) 8612.
[25] M.J. Frisch, G.W. Trucks, H.B. Schlegel, G.E. Scuseria, M.A. Robb, J.R. Cheeseman, J.A. Montgomery Jr., T. Vreven, K.N. Kudin, J.C. Burant, J.M. Millam, S.S. Iyengar, J. Tomasi, V. Barone, B. Mennucci, M. Cossi, G. Scalmani, N. Rega, G.A. Petersson, H. Nakatsuji, M. Hada, M. Ehara, K. Toyota, R. Fukuda, J. Hasegawa, M. Ishida, T. Nakajima, Y. Honda, O. Kitao, H. Nakai, M. Klene, X. Li, J.E. Knox, H.P. Hratchian, J.B. Cross, C. Adamo,

J. Jaramillo, R. Gomperts, R.E. Stratmann, O. Yazyev, A.J. Austin, R. Cammi, C. Pomelli, J.W. Ochterski, P.Y. Ayala, K. Morokuma, G.A. Voth, P. Salvador, J.J. Dannenberg, V.G. Zakrzewski, S. Dapprich, A.D. Daniels, M.C. Strain, O. Farkas, D.K. Malick, A.D. Rabuck, K. Raghavachari, J.B. Foresman, J.V. Ortiz, Q. Cui, A.G. Baboul, S. Clifford, J. Cioslowski, B.B. Stefanov, G. Liu, A. Liashenko, P. Piskorz, I. Komaromi, R.L. Martin, D.J. Fox, T. Keith, M.A. Al-Laham, C.Y. Peng, A. Nanayakkara, M. Challacombe, P.M.W. Gill, B. Johnson, W. Chen, M.W. Wong, C. Gonzalez, J.A. Pople, GAUSSIAN 03, Revision B.05, Gaussian, Inc., Pittsburgh, PA, 2003.

[26] J.L. Lin, W.B. Tzeng, J. Chem. Phys. 115 (2001) 743.
[27] J.L. Lin, C. Li, W.B. Tzeng, J. Chem. Phys. 120 (2004) 10513.
[28] G. Lembach, B. Brutschy, Chem. Phys. Lett. 273 (1997) 421.
[29] J.L. Lin, W.B. Tzeng, J. Chem. Phys. 113 (2000) 4109.
[30] G. Varsanyi, Assignments for Vibrational Spectra of Seven Hundred Benzene Derivatives, New York Academic Press, New York and London, 1974, pp. 161–184.
[31] O. Dopfer, K. Müller-Dethlefs, J. Chem. Phys. 101 (1994) 8508.
[32] C. Li, J.L. Lin, W.B. Tzeng, J. Chem. Phys. 122 (2005) 044311.
[33] M. Gerhards, C. Unterberg, S. Schumm, J. Chem. Phys. 111 (1999) 7966.
[34] E. Fujimaki, A. Fujii, T. Ebata, N. Maikami, J. Chem. Phys. 110 (1999) 4238.
[35] C. Unterberg, A. Gerlach, A. Jansen, M. Gerhards, Chem. Phys. 304 (2004) 237.
[36] B. Zhang, C. Li, H.W. Su, J.L. Lin, W.B. Tzeng, Chem. Phys. Lett. 390 (2004) 65.
[37] C. Li, M. Pradhan, W.B. Tzeng, Chem. Phys. Lett. 411 (2005) 506.
[38] E. Drougas, J.G. Philis, A.M. Kosmas, J. Mol. Struct. (Theochem) 758 (2006) 17.
[39] M. Mineyama, T. Egawa, J. Mol. Struct. 734 (2005) 61.
[40] H.D. Bist, J.C.D. Brand, D.R. William, J. Mol. Spectrosc. 24 (1967) 42.